

Triple junction effects in solids

B. Zhao^a, G. Gottstein^{a,*}, L.S. Shvindlerman^{a,b}

^a *Institut für Metallkunde und Metallphysik, RWTH Aachen University, Aachen, Germany*

^b *Institute of Solid State Physics, Russian Academy of Sciences, Chernogolovka, Moscow District, Russia*

Received 22 December 2010; received in revised form 10 February 2011; accepted 14 February 2011

Available online 21 March 2011

Abstract

The grain boundary–free surface triple line tension and grain boundary triple line tension were investigated in copper using a recently introduced novel approach. The effect of triple line tension on grain growth, Zener drag and Gibbs–Thompson relation was studied. The results showed that the triple line tension has a considerable effect on grain growth, particle–boundary interactions and void shape, especially for nanocrystalline materials.

© 2011 Acta Materialia Inc. Published by Elsevier Ltd. All rights reserved.

Keywords: Grain boundary triple junction; Zener drag; Gibbs–Thompson equation; Triple line energy

1. Introduction

The term “triple line” identifies the intersection of three interfaces, either external interfaces or internal interfaces of bulk materials. Triple lines are differentiated based on the interfaces that are intersecting, e.g. three phase boundaries, three grain boundaries, or one grain boundary and two phase boundaries.

One of the earliest studies of triple junctions in materials was the analysis of a groove formed at the intersection of a grain boundary with a surface [1]. The fact that grain boundary motion can be influenced by a thermal groove [2] is established as textbook knowledge. High-resolution transmission electron microscopy observations have shown that the intersection of a grain boundary with a free surface leads to a reconstruction [3]. This proves the existence of a driving force, which is likely to be related to the existence of a grain boundary–free surface line tension [4].

We have recently designed a method to correctly determine the triple junction line tension [5,6]. The method is based on the equilibrium of four line tensions at their point of intersection—the grain boundary triple line and three

triple lines at the bottom of the thermal grooves of the merging boundaries. The line tension of the grain boundary–free surface triple lines is determined by comparing the dihedral angle at the root of a flat and a curved grain boundary groove.

Grain boundary triple junctions have been recognized recently to constitute another structural element of polycrystals, which can strongly impact microstructural evolution [7–9]. They open up new opportunities to control and to design the grain microstructure of fine-grained and nanocrystalline materials through their effect on recovery, recrystallization and grain growth. Knowledge of the magnitude of the grain boundary line tension can provide a quantitative estimate of the contribution of grain boundary triple junctions to the driving force for grain growth. In this study we will show that the Zener force and the Gibbs–Thompson relation and related phenomena are also affected by the triple line energy.

2. Measurement of triple line tension

The fundamental principle underlying the measurement of triple line tension is the establishment of thermodynamic equilibrium at the intersection of four triple junctions, namely three groove root junctions (triple line between

* Corresponding author.

E-mail address: gottstein@imm.rwth-aachen.de (G. Gottstein).

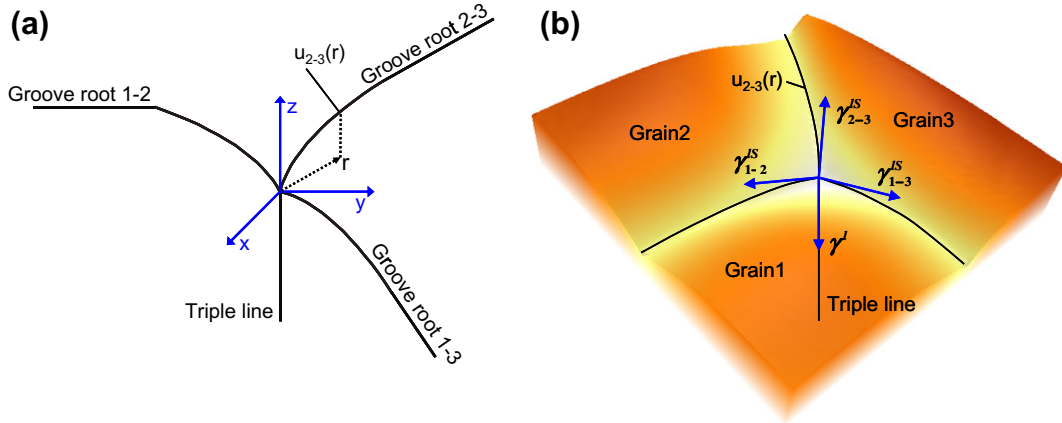


Fig. 1. (a) Schematic 3-D view of the line geometry at a triple junction. (b) AFM 3-D view of the line tension equilibrium at a triple junction [6].

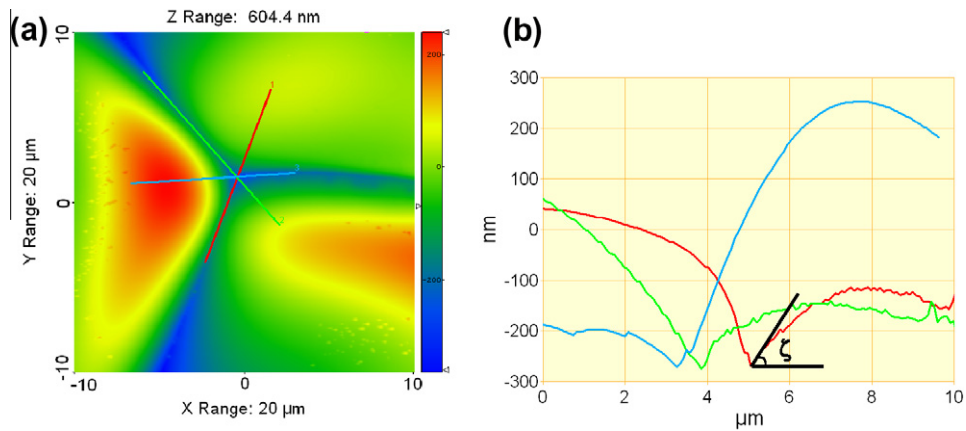


Fig. 2. (a) AFM topography measurement on a triple junction of a Cu tricrystal after annealing at 980 °C for 2 h. (b) Profiles along the lines in (a).

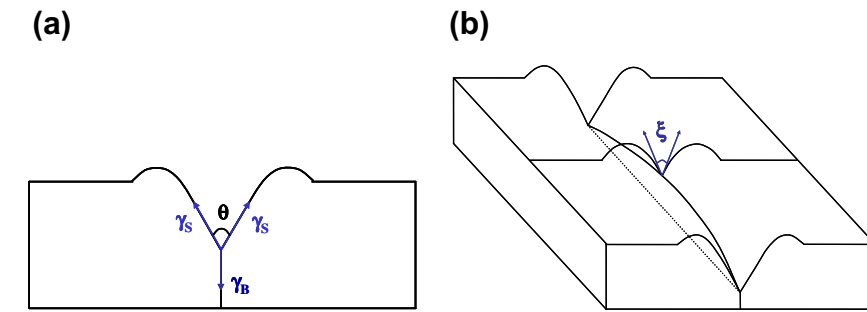


Fig. 3. (a) Grain boundary groove formed at a straight, non-curved grain boundary with no variation in height and (b) grain boundary formed at a flat grain boundary with a curved groove root [6].

two crystal surface and a grain boundary) and one triple junction formed by the intersection of three grain boundaries (Fig. 1).

The equilibrium in the z -direction yields

$$\gamma_{TP}^l = \gamma_{1-2}^{IS} \sin \zeta_{1-2} + \gamma_{1-3}^{IS} \sin \zeta_{1-3} + \gamma_{2-3}^{IS} \sin \zeta_{2-3}, \quad (1)$$

where γ_{TP}^l and γ_{i-j}^{IS} are the grain boundary triple line tension and the line tension of the triple lines at the bottom of each thermal groove, respectively. ζ_{i-j} are the angles at each

groove root of the corresponding grain boundary at the center of the triple junction (Fig. 2).

Eq. (1) requires the determination of the triple line tensions of the groove roots γ_{i-j}^{IS} . This information can be retrieved from the curvature of the groove root triple lines.

Fig. 3a depicts a typical thermal groove formed at a tilt grain boundary which extends perpendicular to the free surface. If the orientation of the surface on both sides of

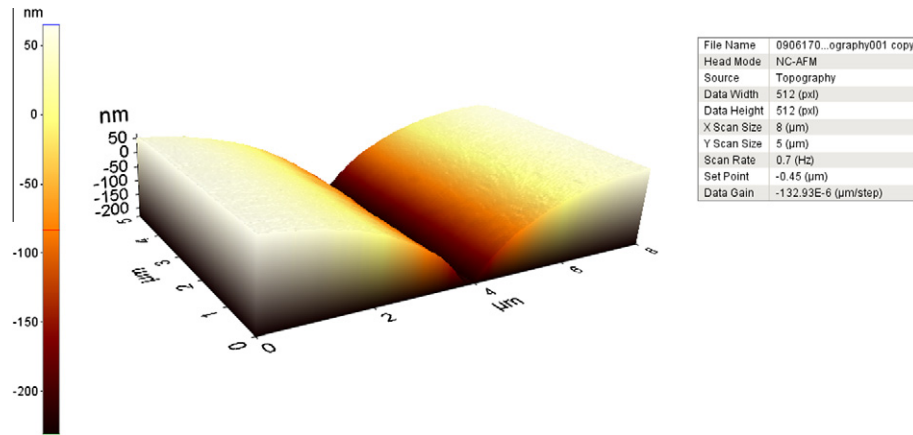


Fig. 4. Top view of AFM topography measurement of a grain boundary groove in a Cu bicrystal after annealing at 980 °C for 2 h.

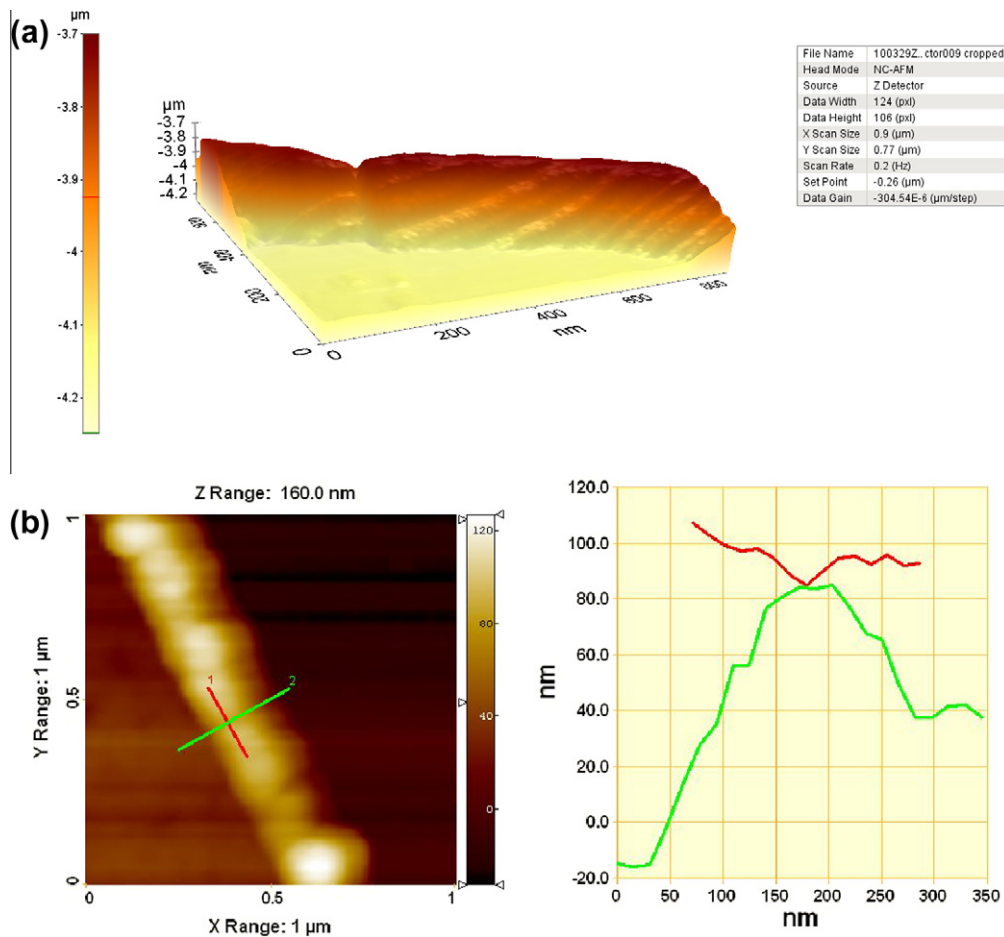


Fig. 5. (a) Top view of AFM topography measurement on a Cu wire after annealing at 300 °C for 2 h. AFM image step size 7 nm. (b) Profiles parallel to and across the thin Cu wire.

the grain boundary is the same and the root of the groove is straight, the specific grain boundary energy is given by:

$$\gamma_B = 2\gamma_S \cos \frac{\theta}{2}, \quad (2)$$

where θ is the dihedral angle at the groove root under the assumption that the grain boundary groove is symmetric, and γ_B , γ_S are the grain boundary tension and the free surface tension, respectively.

The curved groove root in Fig. 3b gives:

$$\gamma_B - \frac{\gamma^{IS}}{R} = 2\gamma_S \cos \frac{\xi}{2}, \quad (3)$$

where R is the radius of curvature at a given point of the groove root. The dihedral angle ξ has the same meaning as θ but may be different in magnitude owing to the curvature. Combining Eqs. (1) and (2) yields the grain boundary–free surface line tension γ^{IS} :

$$\gamma^{ls} = 2\gamma_s \left(\cos \frac{\theta}{2} - \cos \frac{\xi}{2} \right) \cdot R. \quad (4)$$

The measurement of the angle θ was performed on Cu bicrystals with perfect surface quality [6] Fig. 4.

The dihedral angle θ was determined from an atomic force microscopy (AFM) scan perpendicular to the grain boundary groove, and was found to be $\theta = 161.0^\circ \pm 2.3^\circ$. The frequency distribution of the measured dihedral angle was Gaussian.

Measurement of the angle ξ (Eq. (3)) is more difficult. For that, we determined the dihedral angle of the grain boundary groove on very thin Cu wires, which were grown by strain control within thin-film cracks [10] Fig. 5. Copper wire grids were deposited on a silicon substrate, and annealed at 300 °C in a vacuum furnace for 2 h.

To obtain maximum accuracy, the measurements were performed with high-aspect-ratio tips (Olympus AC11160BN-A2) in an atomic force microscope in non-contact mode. The resolution of these tips was calibrated with a tip-check sample, and the geometry of the tip was derived by blind tip reconstruction. According to this calibration, the tip radius was about 10 nm with a slope of 72°. Therefore the step size of the AFM image of Cu wires was also chosen to be ≤ 10 nm for fast and accurate measurement.

The radius of the wire was in the range 80–150 nm. The dihedral angles of the grooves were in the range 150–157° depending on the groove curvature. This yielded on average a line tension of the grain boundary groove root (triple line grain boundary–free surfaces) $\gamma^{ls} = (2.5 \pm 1.1) \times 10^{-8}$ J/m.

Based on the assumptions that

1. the free surface energy is independent of orientation, $\gamma_s = 1.75$ J/m²,
2. the grain boundary–free surface line tension is constant along the groove root, and
3. all grain boundary–free surface line tensions are the same, the grain boundary triple line tension in Cu was determined to be $\gamma_{TP}^l = (6.0 \pm 3.0) \times 10^{-9}$ J/m.

The sign of the grain boundary triple line tension depends on the grain boundary–free surface line tension, which is positive under equilibrium conditions. It was demonstrated in Ref. [6] that a negative grain boundary–free surface line tension would cause the grain boundary–free surface interface to form a convex bulge which would be higher than the surface. Therefore a negative grain boundary–free surface line tension and the normal (classical) shape of a thermal groove system cannot be in equilibrium. Consequently, the grain boundary triple line tension must be positive. This is different from the line tension for a specific system which can undergo a first-order wetting transition, where the line tension will change sign from negative to positive values with increasing temperature [11–13].

Pompe et al. [14] found that the line tension of a three-phase system (solid–liquid–vapor) is of the order of -2×10^{-10} to $+8 \times 10^{-11}$ J/m. The experiments in Ref.

[14] were carried out on hexaethylene glycol, aqueous CaCl₂ solution and water with surface tensions in the range of $(4.5\text{--}7.2) \times 10^{-2}$ J/m². The measured grain boundary–free surface line tension in our experiments on Cu amounted to $\gamma^{ls} = (2.5 \pm 1.1) \times 10^{-8}$ J/m and the respective grain boundary triple line tension was determined to be $\gamma_{TP}^l = (6.0 \pm 3.0) \times 10^{-9}$ J/m with $\gamma_s = 1.75$ J/m² obviously in reasonable agreement with Ref. [14].

3. Impact of triple line tension on grain growth

3.1. Effect of triple junctions on the driving force for grain growth

It was shown in Refs. [15,16] that the influence of grain boundary junctions (triple line and quadruple junction in 3-D polycrystals) on grain growth kinetics can be described in terms of a parameter A . The rate of 3-D grain growth can be expressed as:

$$\frac{d\langle D \rangle}{dt} = \frac{m_B P}{\left(1 + \frac{1}{A_{QP}} + \frac{1}{A_{TP}} \right)}, \quad (5)$$

where D is the grain size, and A_{QP} and A_{TP} are the quadruple point and triple junction parameters, respectively [17]. We note that $\frac{1}{A}$ is a measure of the drag effect of a given junction on grain growth. However, junctions do not only exert a drag on grain boundary motion, but also contribute to the driving force for grain growth due to the junction energy. The classical equation for the driving force P for continuous grain growth reads $P = \frac{2\gamma_B}{R}$. Here, $2/R$ is the grain boundary curvature. If, for simplicity, we assume $R \approx \langle D \rangle$, the total driving force from grain boundaries and triple junctions reads:

$$P = \frac{2\gamma_B}{\langle D \rangle} + \frac{36\gamma_{TP}^l}{\pi \langle D^2 \rangle}. \quad (6)$$

The ratio $\frac{P_{TP}}{P_B} = \frac{18\gamma_{TP}^l}{\pi\gamma_B} = a$ defines the grain size for which the grain boundary and triple junction contributions to the driving force are equal. Assuming the measured value of $\gamma_{TP}^l \approx 6 \times 10^{-9}$ J/m² for Cu, a constant grain boundary surface tension of Cu $\gamma_B = 0.6$ J/m² and a constant ratio γ_{TP}^l/γ_B , we arrive at $a \approx 55$ nm. In other words, up to a mean grain size of about 55 nm the driving force stemming from triple junctions is larger than that of the grain boundaries. As a consequence, a correct examination of grain growth in nanocrystalline materials at least up to mean a grain size a cannot be performed if the driving force of triple junctions is not taken into account [17].

3.2. Effect of triple line tension on grain boundary–particle interaction

In 1948 Zener proposed a concept of how the interaction between a grain boundary and a particle can be estimated quantitatively [18].

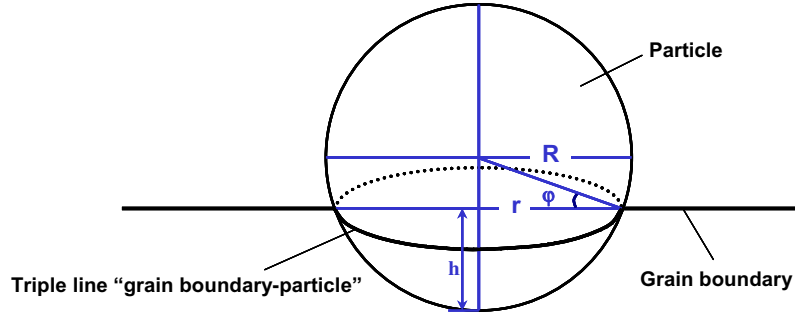


Fig. 6. Schematic view of a particle intersecting a grain boundary.

When a spherical solid particle intersects a grain boundary, it replaces part of the grain boundary area, and by doing so reduces the free energy of the system:

$$\Delta G = -\pi r^2 \cdot \gamma_B, \quad (7)$$

where G is the Gibbs free energy, γ_B is the boundary energy, and r is the radius of the intersected circular area (Fig. 6).

However, this area has to be regenerated when the grain boundary detaches from the particle. The respective retarding force, i.e. the “Zener force”, is given by:

$$f = \frac{d\Delta G}{dr} = -2\pi r \cdot \gamma_B, \quad (8)$$

which retards the motion of the grain boundary.

For the past 60 years all considerations of grain boundary motion and grain growth in solids with both immobile and mobile particles have been based on this concept, i.e. the triple line that forms at the intersection of sphere and boundary was simply disregarded. In Section 2 we showed that a triple line is a defect in its own right with specific thermodynamic properties, and that the line tension of a triple junction can be measured. Hence, such measurements can be utilized to study its effect on particle boundary interaction [19]. Then, Eq. (7) has to be rewritten as:

$$\Delta G_I^0 = -\pi r^2 \cdot \gamma_B + 2\pi r \cdot \gamma^{BP}, \quad (9)$$

where γ^{BP} is the line tension of the triple junction.

Let us define the coefficient $\eta = \frac{\gamma_B \cdot R}{\gamma^{BP}}$.

The derivative of Eq. (9) reads:

$$\frac{d\Delta G_I^0}{d\varphi} = 2\pi R \gamma^{BP} \sin \varphi \cdot (\eta \cos \varphi - 1). \quad (10)$$

For $\eta < 1$, ΔG_I^0 attains a maximum value at $\varphi = 0$. When $\eta > 1$, the maximum shifts to $\cos \varphi = \frac{1}{\eta}$, and ΔG_I^0 assumes a minimum at $\varphi = 0$. The sign of ΔG_I^0 depends on the particle radius, as shown in Fig. 7.

From Eq. (9), we obtain the interaction force between the grain boundary and the particle:

$$F^* = -2\pi r \cdot \gamma_B + 2\pi \gamma^{BP} \quad (11)$$

At the critical particle size $R^* = \frac{\gamma^{BP}}{\gamma_B}$, f^* changes sign. Hence, for $R < R^*$ the particle will not attach to the grain boundary. When the particle radius is larger than R^* , and

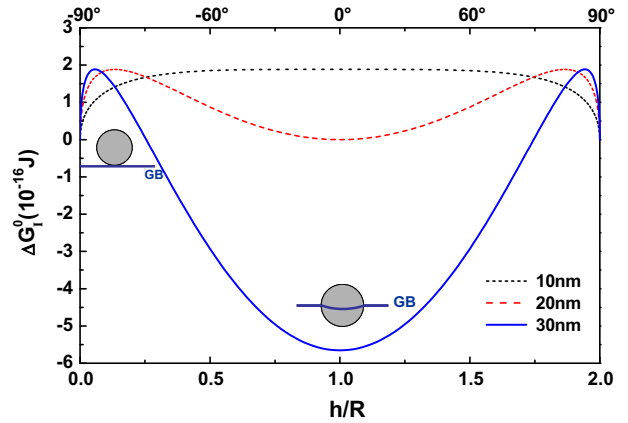


Fig. 7. Dependency of ΔG_I^0 on particle radius in Cu for $\gamma^{BP} = \gamma_{TP}^I$; h is the penetration depth of the boundary in the particle as defined in Fig. 6.

$\varphi < \arccos \frac{1}{\eta}$, the grain boundary would intersect the particle, and f^* becomes a retarding force for grain boundary motion.

In Cu, $\gamma_B = 0.6 \text{ J/m}^2$, and if we assume $\gamma^{BP} \approx \gamma^{IS} = (2.5 \pm 1.1) \times 10^{-8} \text{ J/m}$, the critical size R^* is about 40 nm; if we take the value $\gamma^{BP} \approx \gamma_{TP}^I = (6.0 \pm 3.0) \times 10^{-9} \text{ J/m}$, the critical size R^* is about 10 nm. According to Fig 7, $\Delta G_I^0 > 0$ for $R < R^*$ and increases with growing area of intersection. The minimum value of $\Delta G_I^0(\varphi)$ is obtained at $\varphi = \pm 90^\circ$, therefore the particle will not attach to the grain boundary at all. When $R > R^*$, a further minimum of $\Delta G_I^0(\varphi)$ appears at $\varphi = 0^\circ$. On the other hand, the impact of the triple junction on particle–boundary interaction brings about the formation of an energy barrier. This barrier can only be overcome with the help of an external driving force, as follows:

$$\Delta G_I = -\pi r^2 \cdot \gamma_B + 2\pi r \cdot \gamma^{BP} - PV. \quad (12)$$

The external driving force P will expend a work proportional to the swept volume V . The energy barrier still exists, but the grain boundary will become curved under the driving force. If we assume that the radius of the curved grain boundary is equal to the radius of the particle, the change in the system energy ΔG_C due to the curved grain boundary reads:

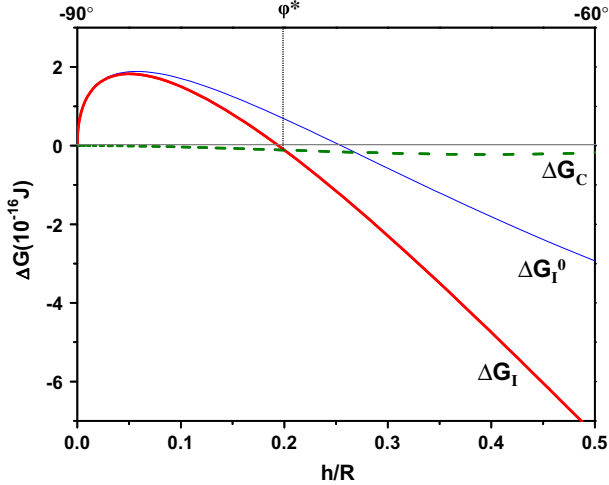


Fig. 8. The dependencies of ΔG_I^0 , ΔG_I and ΔG_C on h/R for $R = 30$ nm, $\gamma^{BP} = \gamma_{TP}^l = (6.0 \pm 3.0) \times 10^{-9}$ J/m.

$$\Delta G_C = -\pi r^2 \cdot \gamma_B + 2\pi R h \cdot \gamma_B - P V. \quad (13)$$

Fig. 8 gives an example of the dependencies $\Delta G_I(\varphi)$ and $\Delta G_C(\varphi)$ for $R = 30$ nm, $P = 25$ MPa. Accordingly, the grain boundary will first circumvent the particle (energy curve ΔG_C , broken line in Fig. 8) until the angle φ^* is reached. Then it will intersect the particle (energy curve ΔG_I , thick solid profile in Fig. 8). The angle φ^* and the critical driving force for the process are:

$$\varphi^* = \arcsin \frac{1 - \eta^2}{1 + \eta^2} \quad (14)$$

$$P_{crit} = \frac{(1 + \eta^2)\gamma_B}{\eta^2 R} \quad (15)$$

A detailed derivation is given in the Appendix A.

When the driving force $P > P_{crit}$, the grain boundary can pass the particle, and the interaction force is given by Eq. (11). The maximum interaction force $f_{max}^* = f^*(R)$ does not depend on the driving force.

In other words, a particle cannot cross a grain boundary spontaneously, but a certain driving force needs to be applied to the grain boundary to overcome the barrier. In the course of the process, the grain boundary first becomes curved and eventually will pass the particle.

So far we have assumed that the particle is immobile. In the following we will dwell on the interaction between moving grain boundary and mobile particles [15,20–23]. Since the mobility of a second-phase particle strongly depends on its size, the problem becomes particularly important for fine-grained and nanocrystalline materials. In Ref. [23] this problem was considered in the framework of the Zener approach for steady-state motion of the boundary–particle system. The latter assumes that the shape of a particle which moves together with a grain boundary changes with the velocity of their joint motion. It is of interest to evaluate the size of such a particle. For joint motion, the velocity of a particle and grain boundary have to be equal:

$$v_B = v_P, \quad (16)$$

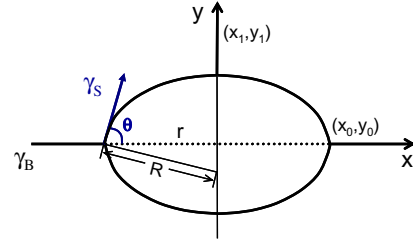


Fig. 9. Schematic view of a void intersecting a grain boundary.

where $v_B = \frac{2m_B\gamma_B}{\langle D \rangle^2}$, and m_B , γ_B and $\langle D \rangle$ are the reduced boundary mobility, grain boundary surface tension and mean grain size, respectively. The particle velocity $v_P = m_P \pi r = \frac{1}{10} \cdot \frac{D_s b \Omega_a}{kT \cdot R^4} \pi R \gamma_B$ [15], where D_s , b , Ω_a and R are the interface diffusion coefficient, lattice constant, atomic volume and particle radius, respectively. For a Cu polycrystal with $\langle D \rangle \approx 10$ $\mu\text{m} = 10^{-5}$ m at 937 K, $\gamma_B = 0.6$ J/m², $D_s \approx 10^{-13}$ m²/s, $b = 3 \cdot 10^{-10}$ m and $\Omega_a = 10^{-5}$ m³/mol, the radius R of a particle moving together with a grain boundary is in the range 1–2 nm. For $R \approx 2$ nm, $\eta = \frac{\gamma_B R}{\gamma_{BP}^l} < 1$ and the critical driving force P for the grain boundary motion which is necessary to permit a second-phase particle to intersect the grain boundary is given by Eq. (15), with parameters $\gamma_B = 0.6$ J/m², $\gamma_{BP}^l \approx \gamma_{TP}^l = 6 \times 10^{-9}$ J/m, $R \approx 2 \times 10^{-9}$ m and $P_{crit} = 7.7 \times 10^9$ J/m³. This value is four orders of magnitude larger than the capillary driving force! Even for a mean grain size $\langle D \rangle \approx 20$ nm the critical driving force P_{crit} is larger than the driving force for grain growth. In other words, the motion of a 2–3 nm particle adsorbed to the moving grain boundary according to the Zener model under a capillary driving force is impossible [23].

3.3. Effect of triple line tension on the Gibbs–Thompson relation

Let us consider the shape of a void at a grain boundary in a polycrystal. For homogeneous materials the contact angle θ is constant, and the equilibrium surface will constitute a surface of rotation [18,19] (Fig. 9). Owing to the symmetry of the problem, the free energy of the system can be expressed as:

$$\Delta G = \int_{y_0}^{y_1} (4\pi x \sqrt{1+x^2}) dy \cdot \gamma_S - \pi x_0^2 \gamma_B + 2\pi x_0 \gamma^{IS}, \quad (17)$$

where γ_S is the free surface energy, γ_B is the grain boundary energy and γ^{IS} is the grain boundary–free surface triple line tension.

Since the volume of the void V is constant:

$$V = 2 \int_{y_0}^{y_1} \pi x^2 dy = const, \quad (18)$$

the problem can be reduced to the isoperimetric problem of calculus of variations:

$$J = \int_{y_0}^{y_1} (4\pi x \gamma_S \sqrt{1+x^2} + 2\lambda \pi x^2) dy - \pi x_0^2 \gamma_B + 2\pi x_0 \gamma^{IS}. \quad (19)$$

The extrema of the function J correspond to the extrema of the function $x(y)$, i.e. the shape of the void, in accordance with the Euler equation:

$$\Phi - x' \Phi_{x'} = C_1 \quad (20)$$

and the transverse conditions:

$$\left| -\Phi_{x'} + \frac{\partial U}{\partial x_0} \right|_{y=y_0} = 0, \quad (21)$$

$$|\Phi - \Phi_{x'} \cdot x'|_{y=y_1} = 0, \quad (21')$$

where $\Phi = 4\pi x \gamma_S \sqrt{1+x'^2} + 2\lambda \pi x^2$ and $U = -\pi x_0^2 \gamma_B + 2\pi x_0 \gamma^{IS}$.

The first transverse condition gives us the relation for the contact angle θ :

$$\cos \theta = \frac{\gamma_B}{2\gamma_S} - \frac{\gamma^{IS}}{2x_0 \gamma^S}, \quad (22)$$

while relation (21') defines the slope of the curve $x(y)$ at the point (x_1, y_1) :

$$x'(y_1) \rightarrow \infty \quad (23)$$

It follows from Eq. (22) that the triple line tension reduces the wetting of the void at a grain boundary. If the surface tension γ_S is isotropic, the void is represented by a lenticular body which is bordered by two spherical surfaces (Eq. (21)).

With respect to V and R , we obtain (Fig. 9):

$$V = 2 \int_{y_0}^{y_1} \pi x^2 dy = 2 \cdot \frac{\pi R^2}{3} (1 - \cos \theta)^2 [3R - R(1 - \cos \theta)] = \text{Const.} \quad (24)$$

$$R = \left[\frac{3V}{2(1 - \cos \theta)^2 (2 + \cos \theta)} \right]^{1/3} \quad (25)$$

$$\Delta G = 4\pi R^2 (1 - \cos \theta) \cdot \gamma_S - \pi R^2 \sin^2 \theta \cdot \gamma_B + 2\pi R \sin \theta \cdot \gamma^{IS}. \quad (26)$$

Let us consider the behavior of a void at a grain boundary in Cu ($\gamma_S = 1.75 \text{ J/m}^2$, $\gamma_B = 0.6 \text{ J/m}^2$, $\gamma^{IS} = (2.5 \pm 1.1) \times 10^{-8} \text{ J/m}^2$). The relation between $\theta|_{\Delta G_{\min}}$ and void radius R is given in Fig. 10. The void will not attach to the grain boundary when $R < 40 \text{ nm}$. With increasing R , the angle θ tends to become constant: $\theta_C = \arccos \frac{\gamma_B}{2\gamma_S}$.

The difference between the pressure inside and outside of the void can be found from classical considerations: a system of constant volume V is subdivided by a curved surface with surface tension γ_S into two parts V_1 and V_2 . In our case the intersection of the curved surface with the grain boundary also forms an additional structural element, the triple line grain boundary–free surface. The change in the free energy F then reads:

$$dF = p_1 dV_1 - p_2 dV_2 + \gamma_S dA + \gamma^{IS} dL, \quad (27)$$

where A is the surface area and L is the length of the triple line, respectively. In equilibrium ($dF = 0$) we arrive at:

$$\Delta p = \gamma_S \frac{dA}{dV} + \gamma^{IS} \frac{dL}{dV}. \quad (28)$$

The first term on the right-hand side equals $\gamma_S \left(\frac{1}{R_1} + \frac{1}{R_2} \right)$, where R_1 and R_2 are the principal radii of curvature; for a spherical void the term reduces to $\frac{2\gamma_S}{R}$. The second term on the right-hand side can be given by $\gamma^{IS} \frac{dL}{dV} = \frac{\gamma^{IS} \sin \theta}{2R^2}$. Fig. 10 gives the equilibrium of the system ($\theta|_{\Delta G_{\min}}$) as a function of the void radius R in Cu. Up to $R \approx 200 \text{ nm}$, $\sin \theta > 0.99$, i.e. Eq. (28) can be expressed to a good approximation as:

$$\Delta p = \frac{2\gamma_B}{R} + \frac{\gamma^{IS}}{2R^2}. \quad (29)$$

Eq. (29) defines the equilibrium concentration of vacancies in the vicinity of a void at the grain boundary:

$$c_V = c_v^0 \exp \left[\frac{\Omega}{kT} \left(\frac{2\gamma_B}{R} + \frac{\gamma^{IS}}{2R^2} \right) \right], \quad (30)$$

where c_v^0 is the vacancy concentration far away from the void, and Ω is the atomic volume.

In Cu, in accordance with our measurements of grain boundary–free surface line tension $\gamma_B = 0.6 \text{ J/m}^2$, $\gamma^{IS} = (2.5 \pm 1.1) \times 10^{-8} \text{ J/m}^2$. For $R \approx 20 \text{ nm}$ the terms $\frac{2\gamma_B}{R}$ and $\frac{\gamma^{IS}}{2R^2}$ are of the same magnitude. Hence, the influence of the grain boundary–free surface line tension will make itself felt in nanoscale microstructures.

3.4. Effect of the sign of the triple line tension

Of particular interest is the problem of the sign of the triple line tension. As shown with good accuracy in Ref. [6], the measured value of the triple line tension in bicrystals and tricrystals is positive. However, there are no physical restrictions preventing the triple line tension from being negative [6,24,25]. As can be seen from Eq. (6), a negative line tension of the grain boundary triple line decreases the driving force for grain growth and, as a consequence,

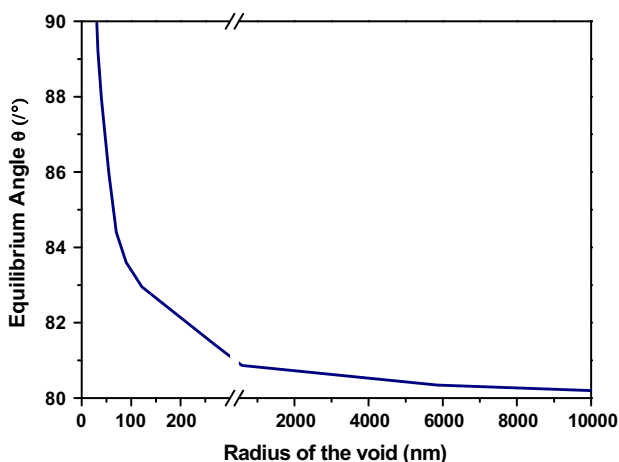


Fig. 10. $\theta|_{\Delta G_{\min}}$ as a function of the void radius R .

stabilizes the grain microstructure: when the line tension “second-phase particle–grain boundary” is negative, the interaction between particle and the grain boundary complies with the Zener approach for all particle sizes (9). If a void is formed at the grain boundary with negative value of γ^{IS} it remains stable and even has to a certain extent the capability to grow (Eqs. (22), (30)). It is most likely that this factor is one reason for the abnormal stability of small voids in nanocrystalline materials [26].

4. Summary

In this study we investigated the effect of triple junctions on a variety of metallurgical phenomena.

1. We detailed how to correctly determine the triple line tension. For Cu, we obtained a tension for the triple line at a groove root of $\gamma^{IS} = (2.5 \pm 1.1) \times 10^{-8}$ J/m, and for the triple line at the intersection of three boundaries $\gamma_{TP}^I = (6.0 \pm 3.0) \times 10^{-9}$ J/m.
2. It was shown that taking into account the grain boundary triple line energy changes fundamentally our understanding of the physics of grain boundary motion and grain growth in nanocrystalline and fine-grained materials, especially in materials with second-phase particles and voids.
3. It was shown that, at least up to a mean grain size of $D \approx \frac{18\gamma_{TP}^I}{\pi\gamma_B}$ (in Cu $D \approx 55$ nm for $D \approx R$), the triple line energy has to be taken into account when calculating the driving force for grain growth in nanocrystalline materials.
4. Based on conditions of thermodynamic equilibrium, the Zener force and the Gibbs–Thompson relation were revisited and modified. To account for the impact of junctions that formed at the intersection of a particle or a void with a grain boundary, we demonstrated that the effect of triple line energy prevents a grain boundary to wet particles and voids if these are smaller than 20–40 nm (in Cu).

Acknowledgements

Financial support of the Deutsche Forschungsgemeinschaft (DFG) through project Go335/35-2 is gratefully acknowledged. We appreciate the financial support of our cooperation through DFG Grant RUS113/846/0-2(R) and the Russian Foundation of Fundamental Research (Grant DFG-RRFI 09-02-91339).

Appendix A

The energy change of a system as the grain boundary intersects a particle is:

$$\Delta G_I^0 = -\pi r^2 \cdot \gamma_B + 2\pi r \cdot \gamma^{BP} \quad (\text{A1})$$

The energy change of the system as the grain boundary circumvents the particle is:

$$\Delta G_C^0 = -\pi r^2 \cdot \gamma_B + 2\pi R h \cdot \gamma_B \quad (\text{A2})$$

Under a constant driving force P :

$$\Delta G_I = -\pi r^2 \cdot \gamma_B + 2\pi r \cdot \gamma^{BP} - PV \quad (\text{A3})$$

$$\Delta G_C = -\pi r^2 \cdot \gamma_B + 2\pi R h \cdot \gamma_B - PV \quad (\text{A4})$$

as

$$\begin{aligned} r &= R \cos \varphi \\ h &= R(1 + \sin \varphi) \end{aligned} \quad (\text{A5})$$

$$V = \pi h^2 (R - h/3) = \frac{\pi R^3}{3} (1 + \sin \varphi)^2 (2 - \sin \varphi)$$

this yields:

$$\begin{aligned} \Delta G_I &= -\pi R^2 \cos^2 \varphi \cdot \gamma_B + 2\pi R \cos \varphi \cdot \gamma^{BP} \\ &\quad - P \cdot \frac{\pi R^3}{3} (1 + \sin \varphi)^2 (2 - \sin \varphi) \end{aligned} \quad (\text{A6})$$

$$\begin{aligned} \Delta G_C &= -\pi R^2 \cos^2 \varphi \cdot \gamma_B + 2\pi R^2 (1 + \sin \varphi) \cdot \gamma_B \\ &\quad - P \cdot \frac{\pi R^3}{3} (1 + \sin \varphi)^2 (2 - \sin \varphi) \end{aligned} \quad (\text{A7})$$

When $\Delta G_{C_min} < 0$, the particle can be encircled by the grain boundary. φ_{C_min} is the position, where ΔG_C has the minimum value.

$$\begin{aligned} \left. \frac{d\Delta G_C}{d\varphi} \right|_{\varphi=\varphi_{C_min}} &= (\pi R^2 \cos \varphi (1 + \sin \varphi) [2\gamma_B \\ &\quad - P \cdot R(1 - \sin \varphi)])|_{\varphi=\varphi_{C_min}} = 0 \end{aligned} \quad (\text{A8})$$

$$\varphi_{C_min} = \arcsin \left(1 - \frac{2\gamma_B}{PR} \right) \quad (\text{A9})$$

$$\begin{aligned} \Delta G_C(\varphi = \varphi_{C_min}) &= \left(\pi R^2 (1 + \sin \varphi)^2 \left[\gamma_B - P \cdot \frac{R}{3} (2 - \sin \varphi) \right] \right)|_{\varphi=\varphi_{C_min}} < 0. \end{aligned} \quad (\text{A10})$$

$$P^* > \frac{\gamma_B}{R} \quad (\text{A11})$$

P^* is the minimum driving force that gets the grain boundary curved by the particle.

The critical angle φ^* , where the grain boundary–particle interaction changes from circumvention to intersection of the particle, is at $(\Delta G_I = \Delta G_C)|_{\varphi=\varphi^*}$:

$$2\pi R \cos \varphi^* \cdot \gamma^{BP} = 2\pi R^2 (1 + \sin \varphi^*) \cdot \gamma_B \quad (\text{A12})$$

Defining the dimensionless coefficient $\eta = \frac{\gamma_B \cdot R}{\gamma^{BP}}$:

$$\varphi^* = \arcsin \frac{1 - \eta^2}{1 + \eta^2} \quad (\text{A13})$$

When φ_{C_min} is smaller than φ^* , the boundary will only bend around the particle. An intersection of the grain boundary with the particle requires $\varphi^* \leq \varphi_{C_min}$. Hence, the driving force P should be:

$$P \geq P_{crit} = \frac{2\gamma_B}{R(1 - \sin \varphi^*)} = \frac{(1 + \eta^2)\gamma_B}{\eta^2 R} \quad (\text{A14})$$

References

- [1] Mullins WW. *J Appl Phys* 1957;28:333.
- [2] Mullins WW. *Acta Metall* 1958;5:414.
- [3] Radetic T, Lancon F, Dahmen U. *Phys Rev Lett* 2002;89:085502.
- [4] King AH. *Mater Sci Technol* 2007;23:505.
- [5] Galina AV, Fradkov VE, Shvindlerman LS. *Fiz Khim Mekh Pov* (Soviet Phys Chem Mech Surf) 1988;1:100.
- [6] Zhao B, Verhasselt Ch J, Shvindlerman LS, Gottstein G. *Acta Mater* 2010;58:5646.
- [7] Czubyko U, Sursaeva VG, Gottstein G, Shvindlerman LS. *Acta mater* 1998;46:5863.
- [8] Gottstein G, Shvindlerman LS. *Z Metallk* 2004;95:219.
- [9] Gottstein G, Shvindlerman LS. *Scripta Mater* 2005;52:863.
- [10] Elbahri M, Jebri S, Wille S, Adelung R. *Adv Solid State Phys* 2009;48:27.
- [11] Bauer C, Dietrich S. *Eur Phys J B* 1999;10:767.
- [12] Pompe T. *Phy Rev Lett* 2002;89:076102.
- [13] Indekeu JO. *Int J Mod Phys B* 1994;8:309.
- [14] Pompe T, Herminghaus S. *Phy Rev Lett* 2000;28:1930.
- [15] Gottstein G, Shvindlerman LS. *Grain boundary migration in metals: thermodynamics, kinetics, applications*. 2nd ed. Boca Raton (FL): CRC Press; 2009.
- [16] Shvindlerman LS, Gottstein G. *Scripta Mater* 2006;54:1041.
- [17] Gottstein G, Shvindlerman LS, Zhao B. *Scripta Mater* 2010;62:914.
- [18] Smith CS. *Trans AIME* 1948;175:175.
- [19] Gottstein G, Shvindlerman LS. *Scripta Mater* 2010;63:1089.
- [20] Gottstein G, Shvindlerman LS. *Acta Metall Mater* 1993;41:3267.
- [21] Novikov V. *Acta Mater* 2010;58:3326.
- [22] Novikov V. *Int J Mater Res* 2007;98:1031.
- [23] Harun A, Holm EA, Clode MP, Miodownik MS. *Acta Mater* 2006;54:3261.
- [24] Gibbs JW. *Trans Connect Acad Arts Sci* 1874;3:289.
- [25] Srinivasan SG, Cahn JE, Jónsson H, Kalonji G. *Acta Mater* 1999;47:2821.
- [26] Estrin Y. Private communication.